DNA Research **17**, 369–379, (2010) doi:10.1093/dnares/dsq025
Advance Access publication on November 8, 2010

Genopal™: A Novel Hollow Fibre Array for Focused Microarray Analysis

Daisuke Okuzaki[1,2,†], Tatsunobu Fukushima[3,†], Takahiro Tougan[2], Tomonori Ishii[4], Shigeto Kobayashi[5], Kazuyuki Yoshizaki[3], Takashi Akita[6], and Hiroshi Nojima[1,2,*]

Department of Molecular Genetics, Research Institute for Microbial Diseases, Suita, Osaka, Japan[1]; DNA-Chip Development Center for Infectious Diseases, Research Institute for Microbial Diseases, Suita, Osaka, Japan[2]; Mitsubishi Rayon Co. Ltd, 1-6-41 Kounann, Minato-ku, Tokyo 108-8506, Japan[3]; Rheumatology and Hematology, Tohoku University Hospital, 1-1 Seiryo, Aoba-ku, Sendai 980-8574, Japan[4]; Juntendo Koshigaya Hospital, 560 Fukuroyama, Koshigaya, Saitama 343-0032, Japan[5] and Center for Advanced Science and Innovation, Osaka University, 3-1 Yamadaoka, Suita, Osaka 565-0871, Japan[6]

*To whom correspondence should be addressed. Tel. +81 6-6875-3980. Fax. +81 6-6875-5192.
E-mail: snj-0212@biken.osaka-u.ac.jp

Edited by Osamu Ohara
(Received 13 July 2010; accepted 25 September 2010; published online 8 November 2010)

Abstract

Expression profiling of target genes in patient blood is a powerful tool for RNA diagnosis. Here, we describe Genopal™, a novel platform ideal for efficient focused microarray analysis. Genopal™, which consists of gel-filled fibres, is advantageous for high-quality mass production via large-scale slicing of the Genopal™ block. We prepared two arrays, infectant and autoimmunity, that provided highly reliable data in terms of repetitive scanning of the same and/or distinct microarrays. Moreover, we demonstrated that Genopal™ had sensitivity sufficient to yield signals in short hybridization times (0.5 h). Application of the autoimmunity array to blood samples allowed us to identify an expression pattern specific to Takayasu arteritis based on the Spearman rank correlation by comparing the reference profile with those of several autoimmune diseases and healthy volunteers (HVs). The comparison of these data with those obtained by other methods revealed that they exhibited similar expression profiles of many target genes. Taken together, these data demonstrate that Genopal™ is an advantageous platform for focused microarrays with regard to its low cost, rapid results and reliable quality.

Key words: focused microarray; Takayasu arteritis; spearman; RNA diagnostics; transcriptome

1. Introduction

Genome-wide expression profiling based on microarray technology is a powerful tool for both basic and clinical research focused on understanding genetic interactions and changes in gene pathways. It also facilitates the identification of genomic biomarkers that correlate with disease classification and with patient responses to drug treatment. For practical diagnostic purposes, however, the currently available general-purpose microarrays have significant drawbacks. Large volumes of data, such as from 40 000 genes or more, are not feasibly managed or analysed. Moreover, the high cost of the microarrays and the compound scanning tools has also hampered the clinical application of microarray systems. In contrast, customized, focused microarrays are advantageous for clinical use because they harbour a substantial, but not overwhelming, number of specific genes that allow researchers and clinicians to evaluate the state of target cells in a relatively inexpensive, rapid, and reliable way.[1] Focused microarrays have been successfully applied to the analysis of human embryonic stem cell differentiation,[2] dopaminergic and glial cell differentiation,[3] transcriptional regulation of the glycome,[4] glyco gene targets with therapeutic potential,[5] gene expression in the mitochondria,[6] oestrogenic activity

† These two authors equally contributed to this work.

of phthalate esters[7] and the cell state of non-small cell lung cancer patients.[8] Unfortunately, the focused microarrays currently available, which are based on the two-dimensional display of oligonucleotides on a glass-based platform, do not offer a substantial economic advantage, reliable quality or the possibility for large-scale production.

We report here the development and practical application of a novel platform for focused microarray, termed Genopal™. The performance of two types of focused microarrays were validated using fluorescently labelled antisense oligonucleotides selected from the genomes of infectious bacteria and viruses for the former, and complementary RNAs (cRNAs) derived from peripheral blood mononuclear cells (PBMCs) of Takayasu arteritis (TA) patients for the latter. TA is a rare autoimmune disease of unknown origin that predominantly affects women and leads to inflammation of the large arteries, resulting in various types of aortoarterial stenosis/occlusion or dilatation.[9,10]. Here, microarray analysis based on the Spearman rank correlation identified an expression pattern specific to TA, which suggests that the Genopal™ is useful for the diagnosis of TA.

2. Patients, Materials and Methods

2.1. Human subjects and ethical considerations

All systemic vasculitis patients used in this study were diagnosed according to a previously documented proposal (the ACR criteria and the CHCC criteria). This study was reviewed and approved by the Internal Review Board of the Research Institute for Microbial Diseases, Osaka University. Accordingly, written informed consent was obtained from all participants before their PBMCs were obtained. Serum samples were consecutively obtained regardless of the patient's symptom, active or inactive phase.

2.2. Production of hollow fibre arrays

Genopal™ consists of hollow fibres impregnated with gel that firmly adheres to the inner walls of the fibres via the introduction of comb polymers (Fig. 1A). Detailed technical aspects of Genopal™ are described in the following patents: US7122378, US20040234114, US20040258897, US2005006 3877 and EP1627839. Briefly, methyl methacrylate (MMA, 100 parts), glycidyl methacrylate (GMA, 100 parts) and azobisisobutyronitrile (AIBN, 0.5 parts) were added dropwise to methyl ethyl ketone (MEK, 50 parts) at 80°C in a nitrogen gas stream (50 ml/min) for 3 h. AIBN (0.1 parts) and MEK (70 parts) were then added, and the mixture was allowed to stand for 1 h. Subsequently, AIBN (0.1 parts) and MEK (10 parts) were added, and the resulting product was allowed to stand for 3 h before the addition of MEK (50 parts). Thereafter, methylhydroquinone (0.5 parts), triphenylphosphine (2.5 parts) and acrylic acid (99 mol % GMA) were added. During these procedures, reactions were aerated (100 ml/min) and allowed to proceed for 30 h. Comb polymers with vinyl groups added to their side-chain termini were obtained. These copolymers contained 25 mol % vinyl groups (Fig. 1B).

Two hundred and twenty-five hollow poly-MMA fibres (outer diameter, 300 μm; inner diameter,

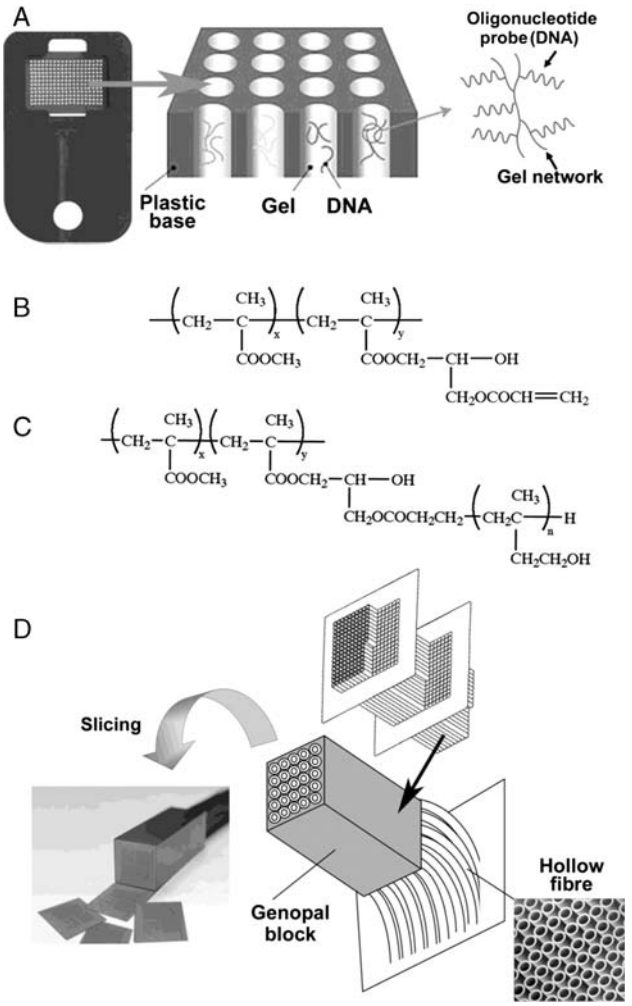

Figure 1. Structure of Genopal™ and its mass production application via slicing of the Genopal™ block. (A) Schematic representation of the Genopal™ microarray, which is composed of plastic hollow fibres. Oligonucleotide DNA capture probes were attached to a hydrophilic gel within the three-dimensional space of each hollow fibre. (B) The chemical structure of the comb polymers containing polymer-forming functional groups on their side chains. These polymers were inserted into the hollow fibres. (C) Comb polymers with poly HEMA added to their side chains firmly adhered to the inner walls of the hollow fibres. (D) Schematic representation of a Genopal™ block: the hollow fibres were bundled in an orderly arrangement, hardened with resin to form a Genopal™ block and sliced into thin microarrays.

200 μm; length, 60 cm; Mitsubishi Rayon Co. Ltd, Tokyo, Japan) were bundled, and comb polymers were introduced into the hollow portions. Part of the solution introduced by suction into the hollow portions was transferred to the trap tube, and the solvent remaining on the inner walls of the hollow portions was allowed to evaporate by air drying. Subsequently, two porous plates (thickness, 0.1 mm) comprising 49 pores each arranged in seven rows in both lengthwise and breadthwise directions, with a pore diameter of 0.32 mm and centre-to-centre distances between neighbouring pores of 0.42 mm, were stacked. Forty-nine hollow fibres of poly-MMA were allowed to pass through each pore of these two porous plates. The distance between the two porous plates was 50 mm, and both ends were immobilized while the threads were stretched between them. The starting material for the resin was then made to flow into the hollow fibre array and allowed to harden. Polyurethane resin adhesives (Nippolan 4276, Coronate 4403; by Nihon Polyurethane Industry Co. Ltd, Shunan-shi, Japan) were used. The porous plates were removed after the resin hardened, producing the resin block containing hollow fibres.

In the final step of the oligonucleotide synthesis, the reaction was performed using Aminolink II (Applied Biosystems, Foster City, CA, USA) to synthesize an oligonucleotide with aminated termini. The resulting GCAT oligo with aminated termini (50 μl, 500 nmol/ml), GMA (5 μl) and dimethylformamide (5 μl) were mixed, and the mixture was allowed to react at 70°C for 2 h before the addition of 190 μl of water. Thus, we obtained a GCAT oligo with 100 nmol/ml methacrylate groups (MA-GCAT). Subsequently, we prepared a starting solution for a gel comprise the monomer and the initiator with the following mass ratios: 9 parts acrylamide, 1 part *N*,*N*′-methylenebisacrylamide, 0.1 part 2,2′-azobis (2-methylpropionamidine)dihydrochloride (V-50) and 90 parts water. MA-GCAT was then added to the above solution to a final concentration of 0.5 nmol/l. The hollow portions of the hollow fibres in the resin block were filled with this solution, the block was transferred into a humidified hermetically sealed glass vessel, and the content of the vessel was allowed to polymerize at 70°C for 3 h. Thus, a block of hollow fibre array in which the hollow portion was impregnated with gel was obtained. This block was sliced to a thickness of 500 μm in a direction perpendicular to the direction of fibres.

2.3. Preparation of infectant and autoimmunity arrays

The infectant Genopal™ probe (iGp) array were comprise 60 nucleotides (nts) from the genome sequences of 40 types of infectious bacteria and viruses (Supplementary Table S1), taking into consideration the specificity, melting temperature, GC content (40–60%) and secondary structure predicted with ProbeQuest software (Dynacom Co., Chiba, Japan). The generated synthetic DNA oligonucleotides were installed onto a Genopal™ platform to keep them immobilized in the hydrophilic gel within the three-dimensional space of each hollow fibre (Mitsubishi Rayon Co. Ltd). To prepare autoimmunity Genopal™ probe (aGp) array, 216 genes were selected based on their relevance to autoimmune diseases (Supplementary Fig. S2A and Table S2), 65 nt Genopal™ probes with similar annealing temperatures were designed, and the oligonucleotides were synthesized and installed onto the Genopal™ platform. Here, we also considered the melting temperature, GC content, specificity, secondary structure and low complexity of the sequences, which were primarily located within 1000 bases of the 3′ end of mRNA sequences.

2.4. RNA isolation

Total RNA from fresh PBMCs of patients and pooled healthy volunteers (HV pools) was isolated using the PAXgene Blood RNA Kit and RNeasy Mini Kit with the optimal on-column DNase digestion, according to the manufacturer's instructions (Qiagen KK, Hilden, Germany). The quality of the RNA samples used for the microarray analysis was examined using the RNA 6000 Nano LabChip Kit (p/n 5067-1511) on the Agilent 2100 Bioanalyzer (G2938C; Agilent Technologies Inc., Palo Alto, CA, USA).

2.5. Microarray analysis on Genopal™

Hybridizations on the infectant and autoimmunity arrays were carried out in 150 μl of hybridization buffer (0.12 M Tris–HCl, pH 7.5, 0.12 M NaCl, 0.05% Tween-20 and the indicated amount of antisense-oligonucleotides or 1125 ng of cRNA) at 65°C overnight or for the indicated times (for time-course measurements; Supplementary Fig. S1B) in a Genopal™-specific hybridization chamber (Mitsubishi Rayon Co. Ltd). After hybridization, the Genopal™ arrays were washed twice in 0.12 M Tris–HCl (pH 7.5), 0.12 M NaCl and 0.05% Tween-20 at 65°C for 20 min, followed by washing in 0.12 M Tris–HCl (pH 7.5), 0.12 M NaCl at room temperature for 10 min. The Genopal™ array was then scanned, and the image was captured using a cooled charge-coupled device type Microarray Image Analyzer equipped with multibeam excitation technology (Yokogawa Electric Co., Tokyo, Japan). For infectant array data, Microsoft Excel was used to calculate the coefficient of variation (CV) between

arrays, between scans and between sections. For autoimmunity array data, signal intensities were processed by Subio Basic Plug-in (v1.6; Subio Inc., Aichi, Japan) as follows. First, all values <1 were replaced by 1 and $\log_2$ transformed. Next, ratios against intensities of the HV pools were calculated. Processed signals from 13 TA samples were averaged by 216 genes to generate a reference TA profile. Finally, the Spearman rank correlation between each sample and the reference TA profile by R were calculated. The details of the microarray data have been deposited in the Gene Expression Omnibus (GEO; www.ncbi.nlm.nih.gov/geo) database (accession number GSE18247).

2.6. Data analysis of aGp array

We obtained raw data by measuring the signal intensity with exposure time of 0.1, 1.0, 4.0, 40 and 120 s. Then, we calculated the values of average, median and standard deviation (SD) for 216 probe and 12 blank wells (background). In most cases, the subtracted value (median value of 216 probes minus median value of background) exceeded the SD value of background. Thus, we employed it as the expression value. If not, we employed the median value of background as the expression value.

2.7. Microarray analysis on Agilent's microarray

Microarray analyses were performed as two-colour hybridizations as described previously.[11] Total RNAs obtained from PBMCs were independently reverse transcribed using oligo-dT primers containing the T7 RNA polymerase promoter sequence to generate cDNAs, which were then subjected to *in vitro* transcription using T7 RNA polymerase to label the cRNAs with Cy3-CTP or Cy5-CTP (Amersham Pharmacia Biotech, Piscataway, NJ, USA) using a Fluorescent Linear Amplification Kit (Agilent Technologies Inc.). Purified Cy5-labelled cRNAs (825 ng) from TA patients were then mixed with an equal amount of reverse-colour Cy3-labelled cRNAs from HV pools. Hybridizations, washing, scanning and gene analysis with Agilent's Whole Human Genome Microarray 4×44K G4112F were conducted according to the manufacturer's protocol (Agilent Technologies Inc.). Agilent Feature Extraction software (v. 9.5.1) was used to assess spot quality and extract feature intensity statistics. The Subio Platform and the Subio Basic Plug-in (v1.6; Subio Inc.) were then used to calculate the log ratio of rProcessedSignal over gProcessedSignal (HV pools). The details of the microarray data have been deposited in the GEO (www.ncbi.nlm.nih.gov/geo) database (accession number GSE18245). Genopal™ and Agilent's Whole Human Genome Microarray 4×44K data reported in this paper have been also deposited as superSeries GSE18316.

2.8. Expression profiling using quantitative reverse transcription–polymerase chain reaction and nCounter™ analyses

Assay-on-Demand TaqMan probes with relevant primers were used for quantitative reverse transcription–polymerase chain reaction (qPCR) analysis using the ABI PRISM 7900 according to the manufacturer's instructions (PE Applied Biosystems). Total RNA (500 ng) obtained using the PAXgene Blood RNA Kit was reverse transcribed with the High Capacity cDNA Archive Kit (ABI). PCR consisted of an initial denaturation (95°C, 10 min) followed by 40 cycles of denaturation (95°C, 15 s) and annealing/extension (60°C, 1 min). A standard curve was generated from the amplification data for each primer using a dilution series of PBMC RNA as the template. Fold-change values were normalized to GAPDH expression levels using the standard curve method according to the manufacturer's protocol. Measurements performed using nCounter™ were conducted by NanoString Technologies Inc. (Seattle, WA, USA).

3. Results

3.1. Basic design of the Genopal™ hollow fibre array

To provide a useful, focused microarray system for RNA diagnostics, we developed a novel platform termed Genopal™, which is comprise a hollow fibre array (Fig. 1). Different from typical glass slide DNA microarrays, which harbour two-dimensionally captured oligonucleotide probes attached to a solid surface, such as glass, Genopal™ consists of hollow gel-filled fibres in which oligonucleotides are uniquely embedded in a three-dimensionally arranged manner (Fig. 1A). The gel, which consists of copolymers containing 25 mol % vinyl groups (Fig. 1B), are firmly adhered to the inner walls of the hollow fibres via the introduction of comb polymers (Fig. 1C). Moreover, thin slices obtained by bundling these hollow fibres and then slicing the bundle exhibited sufficient adhesion between the gel and the inner walls of the hollow fibres (Fig. 1D). A full description of this platform is available online at http://www.mrc.co.jp/genome/e/index.html.

Genopal™ offers a number of advantages in terms of its low-cost, ease of storage, speed and convenience compared with other microarray devices. First, it generates hybridization signals that are suitable for high-precision analysis. The oligonucleotides embedded in Genopal™ are maintained in wet conditions throughout all steps of the experiment, even during scanning, thereby allowing for rapid and easy

microarray assay. Second, it produces a large number of microarrays with comparable quality, because the hollow fibres bundled into a single resin block are sliced perpendicular to the longitudinal direction of the fibres; this property is particularly advantageous for mass production at low cost when commercialized as a clinical tool for RNA diagnostics, reducing the cost down to nearly 10% of the conventional microarrays. Third, it is durable, robust and portable, as the sliced and packaged Genopal™ microarrays are maintained under wet conditions. The comb polymer, in particular, prevents the gel from detaching from the inner walls at the time of slicing or during procedures such as hybridization and washing.

3.2. *Preparation and testing of an infectant array*

To examine the quality of the Genopal™ platform, a focused DNA microarray termed the 'infectant array' was designed based on 40 genes (probes) from infectious bacteria and viruses. To design the microarray probes, oligonucleotides 60 nts in length were selected from the genome sequence of each infectant, taking into consideration the melting temperature, GC content, specificity and secondary structure (Supplementary Table S1). The probes were then chemically synthesized and integrated into four independent sections of the Genopal™ gel to test reproducibility of the assay (Supplementary Fig. S1A). Henceforth, we will refer to each 60 nt oligonucleotide as an iGp and each Genopal™ array with these probes as an iGp array. In parallel, antisense DNA (60 nts) was synthesized for use as target DNA corresponding to each iGp and labelled with a fluorescent dye (Cy5) for efficient detection when hybridized with the infectant array (Fig. 2A).

The hybridized signals were observed with high sensitivity; even signals that were very weak after 1 s of scanning became strong enough for analytical purposes at 4 s, and these signals were saturated at 40 s of scanning (Supplementary Fig. S1A). Four arrays, composed of four independent sections, were scanned four times each. In total, 64 measured values for each probe were analysed (Fig. 2A and Supplementary Fig. S1A). The overall CV of signal intensities was very low (10.6% on average), indicating that the iGp array is a highly reproducible platform comparable with other existing microarray systems (Fig. 2B). Thus, the sources of variance were analysed in detail (Fig. 2C) and the largest source was between arrays (44.7%), as expected. The second largest source was between sections (38.1%), whereas variations between scans were slight (17.3%). Taken together, these results indicate that Genopal™ is a reliable platform for focused microarray that produces reproducible results from synthetic RNA samples.

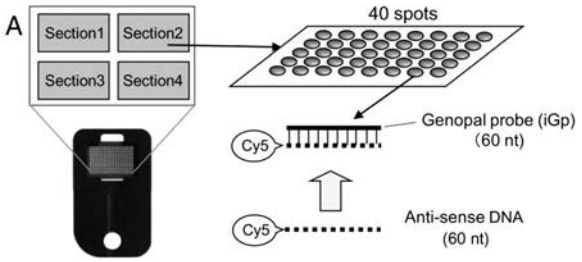

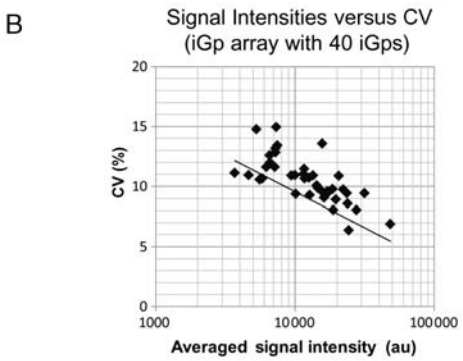

C

Source of variance (% overall variance)	Between arrays 44.7±17.00%	Between scans 17.3±4.57%	Between sections 38.1±16.44%
Experimental structure	Array 1	First scan	Section 1
			Section 2
			Section 3
			Section 4
		Second scan	64 samples in total
		Third scan	
		Fourth scan	
	Array 2		
	Array 3		
	Array 4		

Figure 2. iGp array set-up and data analysis. (A) Experimental design for the use of the iGp array. Each iGp array harboured four identical sets of 40 iGps that contained oligonucleotides (60 nt) corresponding to various infectious bacteria and viruses (Supplementary Table S1). Cy5-labelled antisense DNA (60 nt) was used as a target sample that emitted fluorescent signals when hybridized with the iGps. (B) Scatter plot of averaged signal intensities (horizontal) versus the CV of overall variation (vertical). Four replicate samples were independently prepared for hybridization to four iGp arrays. Each array was scanned four times to obtain 64 measured values for each probe in total. The average signal intensities and CVs were calculated from these 64 values. For each 40 iGps (black diamonds), the CV of the overall 64 average signal intensities (%) was plotted against the original mean value of the calculated average signal intensities. The 75th, 50th and 25th percentile of the CVs (10.1, 11.6 and 11.9%) on the vertical axis and the 75th, 50th and 25th percentile of the average signal intensity (205 032.6, 191 424.1 and 185 480.5 arbitrary units) on the horizontal axis were calculated. (C) Quantification of the sources of variation in the replicated iGp array. Sources of variance between arrays, between scans and between sections, composed of array 1 to array 4, 1st scan to 4th scan, and section 1 to section 4, were calculated to be 44.7 ± 17.00, 17.3 ± 4.57 and 38.1 ± 16.44% as the percent overall variance, respectively.

To examine whether the iGp array was reliable in terms of speed, it was determined whether the hybridization time, which is the most tedious step in any DNA array, could be shortened. Thus, the span of hybridization time was varied from 0.5 h to overnight and compared with the resulting signal intensities (Supplementary Fig. S1B). We found that a 120-s scan after hybridization for only 0.5 h yielded signals that were sufficiently strong for signal profiling, even though the signal was much reduced compared with that of overnight hybridization (Supplementary Fig. S1C). This result further supported the commercial usefulness of Genopal™.

3.3. *Preparation and testing of an autoimmunity array*

To evaluate the clinical applicability of Genopal™, we designed an 'autoimmunity array' based on genes related to autoimmune diseases. For this purpose, we selected 133 autoimmunity-related genes that were previously identified as being up- or down-regulated in PBMCs from patients with various autoimmune diseases (Fig. 3A and Supplementary Table S2), such as systemic lupus erythematosus (SLE),[11] idiopathic thrombocytopenic purpura (ITP),[11] rheumatoid arthritis (RA)[12] and/or vasculitis.[13] In addition, 12 genes from the group of PBMC-specific genes termed PREP (predominantly expressed in PBMC) genes, which are highly expressed in normal PBMCs but not in normal human fibroblasts,[14] and 68 immunity-related genes known to be involved in immune regulation were also used. Genes for α-tubulin, β-tubulin and GAPDH were used as control probes, but not as normalization probes (Fig. 3A). In total, 216 probes were selected, and 65 nt-long oligonucleotides were designed and synthesized from the mRNA sequence of each gene. These probes were termed aGp (Supplementary Table S2: aGp #1–216), and the Genopal™ array performed with these probes was called an aGp array.

Reference cRNA for fluorescence (Cy5) labelling was amplified using a total mRNA pool extracted from 16 HV pools, which was used for hybridization to the aGp array. Each hybridized aGp array was scanned four times to estimate the variability of the data. The average intensities of 54 of the 216 probes were greater than 50 arbitrary units (au), and the CVs of these probes were very small (median = 4.8%); this is surprising considering the high mRNA complexity of clinical samples. In contrast, the CVs of the rest of probes were larger (median was 14.7%), as expected (Fig. 3B). These results indicate that the aGp arrays also yielded reliable data, although aGp arrays that were hybridized with clinical mRNA samples showed lower intensities and larger CVs than iGp arrays that were hybridized with synthetic antisense DNAs.

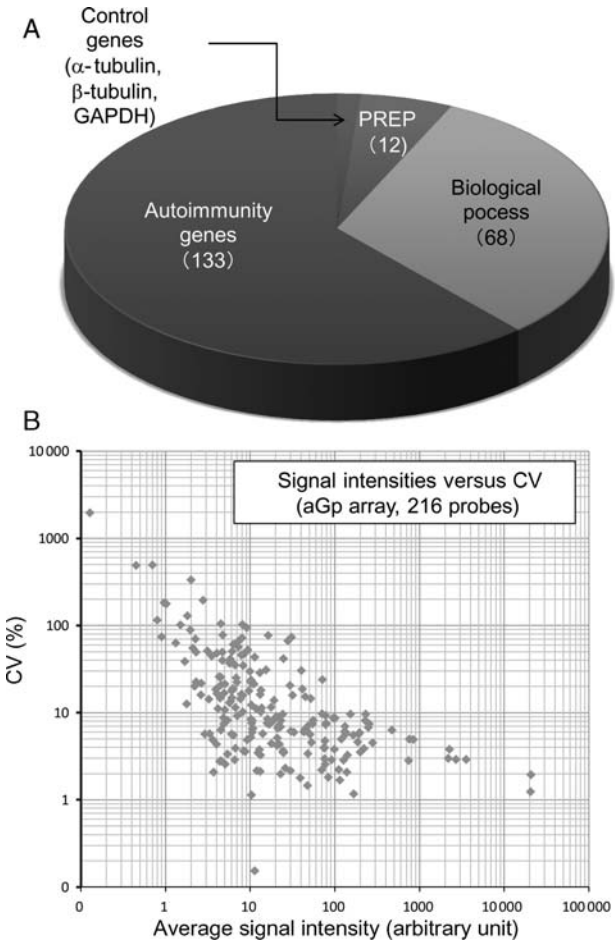

Figure 3. Probe design and execution of aGp arrays. (A) Distribution of the probe groups (autoimmunity-related genes, immunity-related genes, PREP genes and control genes) installed into the aGp array. Each group is indicated by purple, green, red or blue sections, respectively. Among the autoimmunity-related genes, the numbers of up- or down-regulated genes in autoimmune diseases are shown in parenthesis (see the leftmost column of Supplementary Table S2 for details). The probe set of the aGp array is comprise one-third of experimental probes (data not shown) and two-thirds of genes associated with immunity. (B) Scatter plot of average signal intensities (horizontal) and CV (vertical) of the HV pool measured by the aGp array. RNA was extracted from the PBMCs of the HV pool and hybridized onto the aGp array. For 216 aGps on the aGp arrays, the CVs of the average signal intensities measured four times were plotted against the mean calculated average signal intensities. The 216 aGps are represented by grey diamonds. The average, 75th, 50th and 25th percentiles of the CVs (31.3, 22.5, 8.2 and 4.4%) on the vertical axis and the average, 75th, 50th and 25th percentiles of the average signal intensity (288.7, 49.3, 11.3 and 5.3) on the horizontal axis were calculated.

3.4. *Application of the autoimmunity array to clinical samples*

Next, an aGp array was applied to patient samples. Fluorescently labelled cRNAs were prepared using

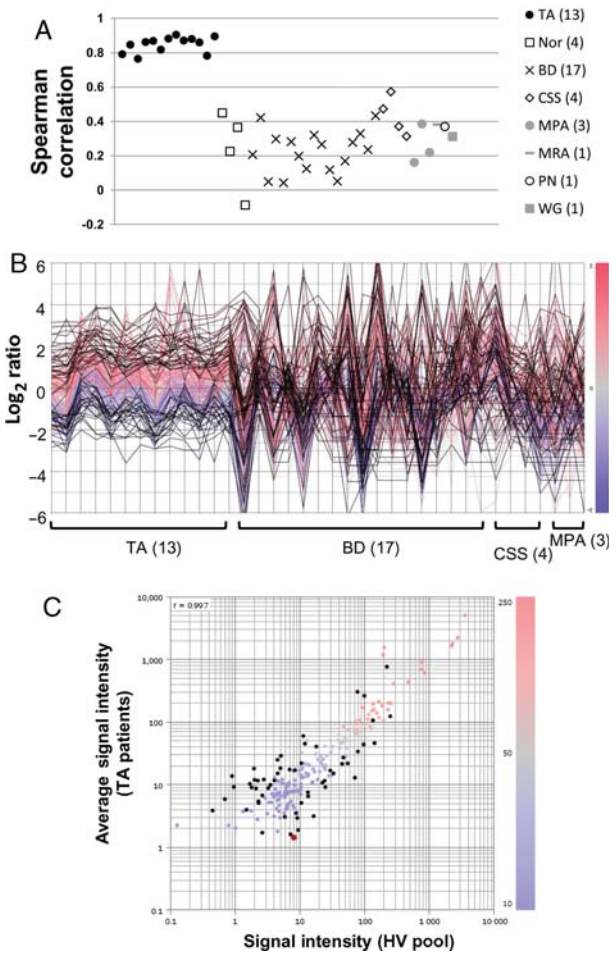

Figure 4. Expression profiling with the aGp array. (A) Comparison of the Spearman rank correlation (vertical) between various autoimmune diseases and normal individuals. Black circles, TA; white squares, Nor (normal); black crosses, BD; white diamonds, CSS; grey circles, MPA; a grey bar, MRA; a white circle, PN; a grey square, WG. The number of tested individuals is indicated in parentheses. Plots are grouped into eight autoimmune disease groups and a HV (Nor) group. All of the 13 TA patients (black circles) are highly correlated by the Spearman rank correlation ($r = 0.85 \pm 0.04$), whereas other autoimmune disease groups and the HV pool group showed distinctively lower correlation coefficients (Nor, 0.24; BD, 0.23; CSS, 0.43; MPA, 0.26; MRA, 0.38; PN, 0.37; WG, 0.31). (B) Line graphs showing the expression profiles of 59 characteristic genes in patients with TA,[13] BD, CSS[4] and MPA.[3] The number of examined patients is indicated in parentheses. The colour bar at the right side of the panel indicates the $\log_2$ ratio for each patient versus the HV pool sample. Line colours with intensity gradients indicate the mean values of relative expression: blue (down-regulation) corresponds to a $\log_2$ ratio -2, and crimson (up-regulation) corresponds to a $\log_2$ ratio 2 when each patient and HV pool are compared. Black lines signify genes that are 2-fold up- or down-regulated in at least 7 of the 13 TA patients compared to the HV pool sample (see Supplementary Table S4 for details). (C) Scatter plot of the average signal intensities (in log scale) of the 13 TA patients versus the HV pool sample, plotted along the vertical and horizontal axes, respectively. Black spots indicate the 59 characteristic genes described above. The colour bar indicates the signal intensity of the 13 TA patients versus the HV pool sample. Circle colours with intensity gradients indicate the mean value of the expression level: blue (down-regulation) corresponds to a signal intensity of 10, and crimson (up-regulation) corresponds to a signal intensity of 250 when the average value of the 13 TA patients and the HV pool are compared. Black circles signify genes that are 2-fold up- or down-regulated in at least 7 of the 13 TA patients compared with the HV pool sample (see Supplementary Table S4 for details).

PBMCs collected from 13 patients suffering from TA, a rare autoimmune disease of the large arteries, and used as target samples. These patients (TA1−13) were under medical care (being treated with anti-inflammatory drugs such as steroids) and were clinically inactive (see Supplementary Table S3 for the patients' morbid states). The 13 TA cRNA samples were hybridized to 13 aGp arrays to generate 13 biological replicates. Additionally, the TA aGp arrays were also tested with other autoimmune diseases such as Behçet's syndrome (BD), Churg−Strauss syndrome (CSS), microscopic polyangiitis (MPA), malignant RA (MRA), polyarteritis nodosa (PN) and Wegener's granulomatosis (WG), as well as with normal volunteers (Nor) as comparable target samples (Supplementary Fig. S2) in order to determine whether the expression profiles of the 13 TA patients were specific and useful for the diagnosis of TA.

To validate the reference TA profile described above by averaging 13 TA samples, the Spearman rank correlation for 216 aGp genes was calculated between each sample and the reference TA profile. Notably, all TA samples (TA1−13) were highly correlated (0.85 ± 0.04) with the TA reference (black circles in Fig. 4A). The maximum and the minimum values of the Spearman rank correlation were computed to be 0.91 and 0.77, respectively, revealing an extremely tight correlation between all TA samples (TA1−13). Moreover, as shown by grey and white symbols in the middle and the right areas of Fig. 4A, other patient samples showed conspicuously low Spearman's rank correlation coefficients (0.29 ± 0.12). This indicates that the aGp array is useful for the diagnosis of TA even if the patient's morbid state is inactive.

Next, 34 genes were isolated that showed at least a 2-fold up-regulation and 25 genes that showed at least a 2-fold down-regulation in at least 7 of 13 TA patients (Supplementary Table S4). We also found that the expression profiles of 59 characteristic genes represented by line graphs in 13 TA, 17 BD, 4 CSS and 3 MPA patients distinguished TA from other autoimmune diseases. The black lines signifying genes that were 2-fold up- or down-regulated in at least 7 of the 13 TA patients randomly fluctuated in other patients (Fig. 4B). Because we did not normalize the aGp array data, systematic shifts in log-ratio distributions in proportion to the signal intensities were observed in the scatter plot (Fig. 4C). Nonetheless,

these 59 genes formed distinctive groupings in terms of correlation across the 216 genes. Namely, up- or down-regulated genes (black circles in Fig. 4C) localized outside the diagonal bundles of dots (purple and crimson circles in Fig. 4C) over a wide range of intensities. In contrast, these 59 genes showed no obvious correlation patterns in other patient samples (data not shown).

Notably, the aGp array has additional practical advantages for clinical use because the obtained data were found to be very stable after scanning, even without sealing or other direct countermeasures against exposure to ozone (Supplementary Fig. S3). Moreover, the background level of the data after 19–27 days were largely reduced compared with 1 day data, which confirmed the reliability of the data even with low signal intensity. Taken together, these results indicate that aGp arrays are clinically useful because they can clearly distinguish TA patient profiles from other patients by the Spearman rank correlation using all 216 probes.

3.5. *Comparison between aGp array, Agilent's microarray and qPCR*

Next, the performance of aGp arrays was compared with other tools to examine the variation of the expression patterns of the genes in the 13 TA patient samples. First, all TA samples (TA1–13) were applied to Agilent's Whole Human Genome Microarray (4 × 44K). DEFA3, interleukin (IL)-4 and IL-10 were selected for further analysis because they are known to be highly associated with various autoimmune diseases.[14] When the expression profiles of each gene from aGp array, Agilent's microarray and qPCR are compared, represented by green, purple and blue lines, respectively, it is apparent that DEFA3 achieved almost complete correlation among the three measurement systems (Fig. 5A). This correlation is surprising considering the distinct sequences of the probes used in each measurement and further confirmed the reliability of the data obtained by aGp arrays. In contrast, IL-4 and IL-10 showed distinct expression patterns depending on the system (Fig. 5Bi and ii).

Notably, IL-4 and IL-10 were expressed at remarkably low levels compared with DEFA3 (indicated by arrows in Fig. 6A). The scatter plot of log signal intensities from the HV pool (horizontal) and patient TA8 (vertical) show that the signal intensities of IL-4 and IL-10 are considerably lower than that of DEFA3. In addition, the correlation coefficients of DEFA3 for the averaged signal intensities of the aGp array and Agilent's microarray against qPCR normalized to GAPDH (0.93 and 0.96) are significantly higher than those of IL-4 (−0.52 and 0.52) and IL-10 (0.12 and −0.06), respectively (Fig. 6B).

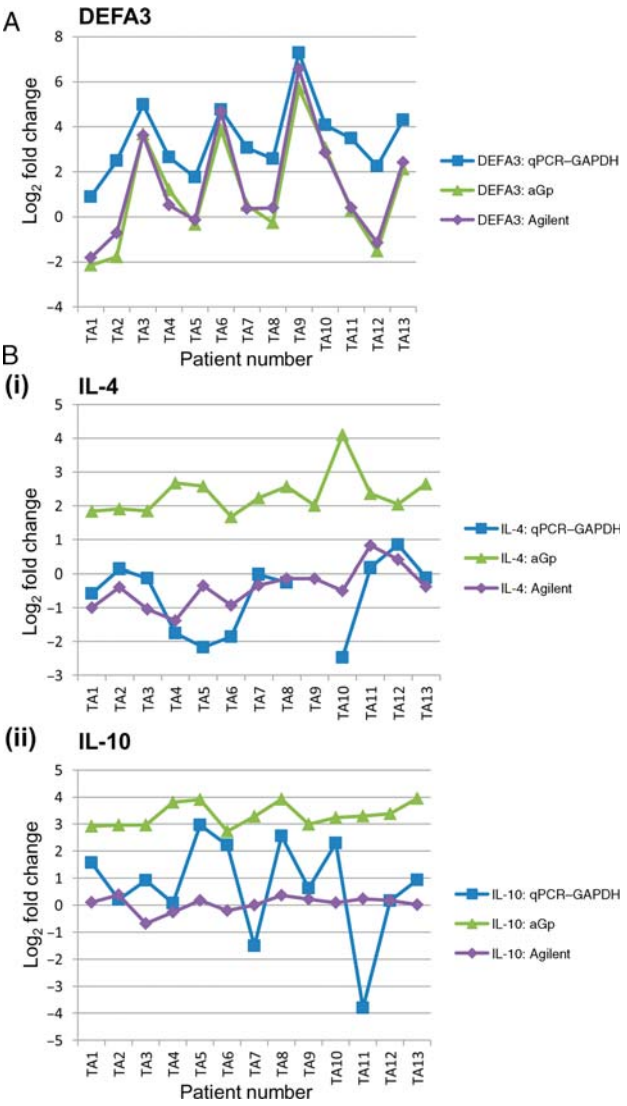

Figure 5. Expression profiles of DEFA3 (A), IL-4 (Bi) and IL-10 (Bii) in the 13 TA patients. The vertical axis indicates the $\log_2$ ratio measured by qPCR–GAPDH (blue), aGp array (green) and Agilent's microarray (purple). The horizontal axis indicates the patient number. (A) The comparison of the values of peaks and valleys for DEFA3 revealed that these three methods yielded very similar expression profiles. (Bi and ii) The expression profiles of the IL-4 and IL-10 genes for the 13 TA patients were different between qPCR–GAPDH (blue), aGp array (green) and Agilent's microarray (purple).

3.6. *Comparison with nCounter™*

To investigate whether aGp or Agilent provided more reliable results, we employed nCounter™ by NanoString[15] and measured the expression levels of 25 relevant genes (aGps) using one patient sample (TA8). The raw data revealed that the expression levels of IL-4 and IL-10 in this patient were very low

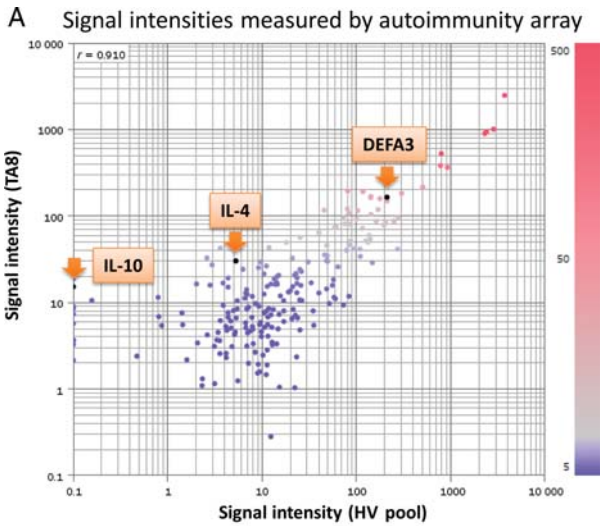

B

	Probe	Correlation coefficient	Average of signals	
			HV pool	TAs
aGp	IL-4	−0.52	5.10	29.00
	IL-10	0.12	−0.76	10.53
	DEFA3	0.93	199.45	1534.39
Agilent	IL-4	0.52	17.15	13.55
	IL-10	−0.06	17.65	18.36
	DEFA3	0.96	58 208.93	277 417.99

Figure 6. The aGp array provides sufficient sensitivity for diagnostic application. (A) A scatter plot of the log of signal intensity of the HV pool versus patient TA8 is plotted along the horizontal and vertical axes, respectively. DEFA3, IL-4 and IL-10 genes are indicated by orange arrows. The attached colour bar indicates a relative intensity scale. (B) The correlation coefficients of the Genopal™ autoimmunity array and Agilent's microarray against qPCR are shown. The correlation coefficient of DEFA3 for both Genopal™ and Agilent's arrays was high. On the other hand, because the signal intensities of IL-4 and IL-10 were within two orders of magnitude, as shown in the columns on the right, the correlation coefficient of IL-4 or IL-10 is lower than DEFA3.

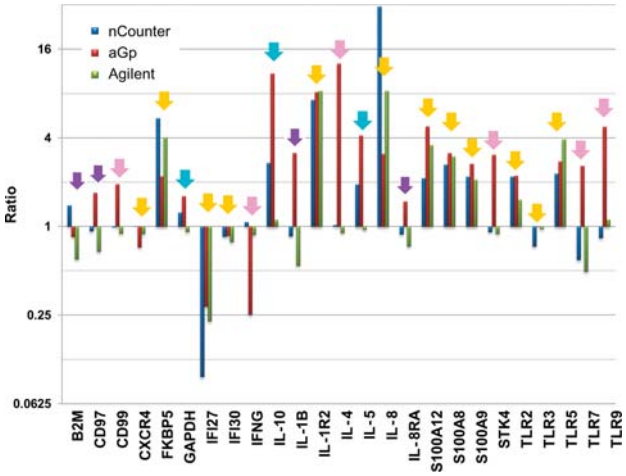

Figure 7. Comparison of the mRNA expression levels (*y*-axis) of 25 selected genes (*x*-axis) in PBMCs of patient TA8 using nCounter™ (blue bars), aGp array (Genopal™; red bars) or Agilent's microarray (green bars). Yellow arrows indicate genes that had similar expression levels in the three methods. Turquoise or pink arrows indicate the genes used by nCounter™ to favour aGp or Agilent in terms of their expression levels. Purple arrows indicate the genes that exhibited different expression levels among the three methods.

and that 10 of the 25 genes were up-regulated more than 2-fold compared with the HV sample (green arrows in Supplementary Fig. S4). Comparison of the relative induction rates between aGp, Agilent and nCounter™ revealed that 12 of the 25 genes (yellow arrows in Fig. 7) had similar results in all three methods, whereas nCounter™ favoured aGp arrays (turquoise arrows) or Agilent (pink arrows) for three and the six genes, respectively. The other four genes (purple arrows) showed distinct results among these three methods. As both nCounter™ and qPCR favoured aGp arrays for IL-10 and Agilent for IL-4 (Supplementary Fig. S5), it is difficult to determine at present which microarray provided more reliable results. Taken together, these results led us to conclude that aGp arrays provide reliable data at a level similar to Agilent's microarray, particularly when the expression levels of the target gene are not very low.

4. Discussion

In the present study, we describe a novel platform termed Genopal™ that is ideal for the preparation of focused microarray (Fig. 1). We first designed the iGp array, examined its performance using Cy5-labelled synthetic oligonucleotides as hybridization probes (Fig. 2A) and determined that it yielded highly reproducible data (Fig. 2B; CV was 10.6% on average). We also prepared the aGp array and tested their clinical applicability using RNA samples from a small volume of PBMCs obtained from TA patients (Fig. 3B and Supplementary Table S3). We do not exclude the usefulness of other genes that were not installed into the aGp array. Nonetheless, we showed that the aGp array is able to distinguish TA patient profiles from HVs and patients with other autoimmune diseases based on the Spearman rank correlation using all 216 probes (Fig. 4). Notably, this data-processing protocol is quite simple and extensible; all that is needed is to calculate the ratio of the Spearman rank correlation for the patients' and HV pool samples. This protocol is useful only for analysis of small number of genes and cannot be applied to conventional genome-wide microarrays, which is another advantageous point of Genopal™. Comparison of the data obtained by an aGp array, Agilent's microarray, qPCR and nCounter™ indicated that these methods exhibited similar expression profiles with regard to target genes with high signal intensities (Figs 5–7).

Using aGp arrays, we also identified here over 10 genes that were up- or down-regulated in almost all TA patients tested (Supplementary Table S4). Among the up-regulated genes, S100A8, S100A9 and S10012 are inflammation-related genes. This is not unexpected because TA is an autoimmune disease that involves enhanced inflammation of the aorta. The up-regulation of amphiregulin (AREG), which is a member of the epidermal growth factor family, may be related to the ventricular hypertrophy often observed in TA patients. Alternatively, it may be involved in the maintenance of inflammatory situations by inducing the proliferation of regulatory cells in these phenomena. Enhanced expression of IL-1 receptor, type II (IL-1R2), a decoy receptor that traps pro-inflammatory IL-1β and does not initiate subsequent signalling events, may be due to a negative feedback response to the hyperactive inflammation in the aorta of TA patients (which results partially from steroid therapy). Defensins, which include DEFA3, are a family of microbicidal and cytotoxic peptides that are abundant in the granules of neutrophils and are thought to be involved in host Defence, which suggest the involvement of infection in the pathogenesis of TA. In contrast, interferon gamma (IFN-G) and interferon-induced genes (G1P2, IFI44, IFIT1, IFIT2 and IFI27) were down-regulated in many TA patients, which distinguish TA from SLE and ITP, as these genes are up-regulated in the latter autoimmune diseases. As there is no reliable diagnostic tool for TA at present, these genes may also be useful as diagnostic markers of the disease when used in combination with the Spearman rank correlation method described above.

One of the practical applications of iGp and aGp arrays would be their use in the diagnosis of patients afflicted with fever of unknown origin (FUO). Our proposal is presented schematically in Supplementary Fig. S6. Namely, a 2-ml blood sample may be collected for every new FUO patient using PAXgene Blood RNA Kits of Quiagen, total RNA prepared, labelled with Cy5 and applied to an aGp array. As the aGp array harbours genes that are either up- or down-regulated in the PBMCs of several autoimmune diseases, such as SLE,[11] ITP,[11] RA[12] and/or vasculitis,[13] we expect to observe positive signals if the patient's FUO is related to any of these autoimmune diseases. In this case, the FUO patient may be directly referred to an autoimmune disease specialist to receive appropriate care. If the screen yielded negative results, other sample sources, such as phlegm and/or excrement, depending on the dubious infectants, may be collected for RNA preparation and screening using the iGp array. If a positive signal is detected, the patients could then be treated appropriately at the bedside. Recent reports indicate that Genopal™ is useful not only for cRNA but also for miRNA samples.[16–20]

Taken together, we conclude that Genopal™ is an advantageous platform for focused microarrays with regard to its low cost, reliability, ease of storage, speed and suitability for large-scale production. The data-processing protocol we developed here might be quite useful for the diseases that lack diagnostic tools using conventional clinical methods.

Acknowledgements: We thank Dr Claudia Gaspar of Bioedit Ltd. for critically reading this manuscript. We also thank Dr Akio Tanabe of Subio Inc. for technical advice in data analysis, Ms Maki Fukuda and Ms Chiharu Nakashima of our laboratory for technical assistance in microarray experiments, Mr Kazuhiko Yuyama of Gene Design Inc. for the synthesis of Genopal™ probes and Dr Nathan Elliott of NanoString Technologies Inc. (Seattle, WA, USA) for the nCounter™ analysis

Supplementary Data: Supplementary Data are available at www.dnaresearch.oxfordjournals.org.

Authors' contributions

D.O. and T.F. designed and performed research, T.T. performed research on the infectant array, T.I. and S.K. provided TA patient samples and monitored the results, T.A. developed the Genopal™ system and H.N. designed the research and wrote the manuscript. K.Y. provided BD samples.

Funding

This work was supported in part by grants-in-aid from the Bio-Medical Cluster Project In Saito, Innovation Plaza Osaka and the Regional Research and Development Resources Utilization Program of the Japan Science and Technology Agency (JST); and Scientific Research on Priority Areas Applied Genomics, Scientific Research (S), Exploratory Research and the Science and Technology Incubation Program in Advanced Regions from the Ministry of Education, Culture, Sports, Science and Technology of Japan to H.N.

References

1. Wurmbach, E., Yuen, T. and Sealfon, S.C. 2003, Focused microarray analysis, *Methods*, **31**, 306–16.

2. Yang, A.X., Mejido, J., Luo, Y., et al. 2005, Development of a focused microarray to assess human embryonic stem cell differentiation, *Stem Cells Dev.*, **14**, 270–84.
3. Luo, Y., Schwartz, C., Rao, M.S., et al. 2006, A focused microarray to assess dopaminergic and glial cell differentiation from fetal tissue or embryonic stem cells, *Stem Cells*, **24**, 865–75.
4. Comelli, E.M., Head, S.R., Gilmartin, T., et al. 2006, A focused microarray approach to functional glycomics: transcriptional regulation of the glycome, *Glycobiology*, **16**, 117–31.
5. Kroes, R.A., Dawson, G. and Moskal, J.R. 2007, Focused microarray analysis of glyco-gene expression in human glioblastomas, *J. Neurochem.*, **103**, 14–24.
6. Voss, J.G., Raju, R., Logun, C., et al. 2008, A focused microarray to study human mitochondrial and nuclear gene expression, *Biol. Res. Nurs.*, **9**, 272–9.
7. Parveen, M., Inoue, A., Ise, R., Tanji, M. and Kiyama, R. 2008, Evaluation of estrogenic activity of phthalate esters by gene expression profiling using a focused microarray (EstrArray), *Environ. Toxicol. Chem.*, **27**, 1416–25.
8. Tanney, A., Oliver, G.R., Farztdinov, V., et al. 2008, Generation of a non-small cell lung cancer transcriptome microarray, *BMC Med. Genomics*, **1**, 20.
9. Ogino, H., Matsuda, H., Minatoya, K., et al. 2008, Overview of late outcome of medical and surgical treatment for Takayasu arteritis, *Circulation*, **18**, 2738–47.
10. Bleeker-Rovers, C.P., van der Meer, J.W. and Oyen, W.J. 2009, Fever of unknown origin, *Semin. Nucl. Med.*, **39**, 81–7.
11. Ishii, T., Onda, H., Tanigawa, A., et al. 2005, Isolation and expression profiling of genes upregulated in the peripheral blood cells of systemic lupus erythematosus patients, *DNA Res.*, **12**, 429–39.
12. Nakamura, N., Shimaoka, Y., Tougan, T., et al. 2006, Isolation and expression profiling of genes upregulated in bone marrow-derived mononuclear cells of rheumatoid arthritis patients, *DNA Res.*, **13**, 169–83.
13. Kobayashi, S., Okuzaki, D., Nojima, H., et al. 2008, Expression profiling of PBMC-based diagnostic gene markers isolated from vasculitis patients, *DNA Res.*, **15**, 253–65.
14. Tougan, T., Onda, H., Okuzaki, D., Kobayashi, S., Hashimoto, H. and Nojima, H. 2008, Focused microarray analysis of peripheral mononuclear blood cells from Churg-Strauss syndrome patients, *DNA Res.*, **15**, 103–14.
15. Geiss, G.K., Bumgarner, R.E., Birditt, B., et al. 2008, Direct multiplexed measurement of gene expression with color-coded probe pairs, *Nat. Biotechnol.*, **26**, 317–25.
16. Hohjoh, H. and Fukushima, T. 2007, Marked change in microRNA expression during neuronal differentiation of human teratocarcinoma NTera2D1 and mouse embryonal carcinoma P19 cells, *Biochem. Biophys. Res. Commun.*, **362**, 360–7.
17. Lee, N.S., Kim, J.S., Cho, W.J., et al. 2008, miR-302b maintains "stemness" of human embryonal carcinoma cells by post-transcriptional regulation of Cyclin D2 expression, *Biochem. Biophys. Res. Commun.*, **377**, 434–40.
18. Kobori, M., Nakayama, H., Fukushima, K., et al. 2008, Bitter gourd suppresses lipopolysaccharide-induced inflammatory responses, *J. Agric. Food. Chem.*, **56**, 4004–11.
19. Takahashi, N., Sato, N., Takahashi, S. and Tojo, A. 2008, Gene-expression profiles of peripheral blood mononuclear cell subpopulations in acute graft-vs-host disease following cord blood transplantation, *Exp. Hematol.*, **36**, 1760–70.
20. Oue, N., Sentani, K., Sakamoto, N., et al. 2009, Characteristic gene expression in stromal cells of gastric cancers among atomic-bomb survivors, *Int. J. Cancer*, **124**, 1112–21.